Tribology International 44 (2011) 1281–1288

Contents lists available at ScienceDirect

Tribology International

journal homepage: www.elsevier.com/locate/triboint

Evaluation of adhesion/cohesion bond strength of the thick plasma spray coatings by scratch testing on coatings cross-sections ☆

Aleksandar Vencl [a,*], Saioa Arostegui [b], Gregory Favaro [b], Fatima Zivic [c], Mihailo Mrdak [d], Slobodan Mitrović [c], Vladimir Popovic [a]

[a] Mechanical Engineering Faculty, University of Belgrade, Kraljice Marije 16, 11120 Belgrade 35, Serbia
[b] CSM Instruments SA, Rue de la Gare 4, CH-2034 Peseux, Switzerland
[c] Mechanical Engineering Faculty, University of Kragujevac, Sestre Janjić 6, 34000 Kragujevac, Serbia
[d] IMTEL Microwaves Inc., Bulevar Mihaila Pupina 165b, 11070 Belgrade, Serbia

ARTICLE INFO

Article history:
Received 2 February 2011
Received in revised form
1 April 2011
Accepted 4 April 2011
Available online 12 April 2011

Keywords:
Plasma spray coating
Bond strength
Scratch test
Tensile test

ABSTRACT

The possibility of adhesion/cohesion bond strength evaluation of thick plasma spray coatings with scratch tester, according to the ISO working draft (ISO/WD 27307), was analyzed and compared with the standard test method (ASTM C 633). Four different coatings deposited with atmospheric plasma spraying were used. The results showed that scratch testing could be used as an efficient method for evaluation of thick plasma spray coatings cohesion. It is a relatively easy and quick test method, and for practical application it could be also used as a supplement of some standard test method as a coating characterization and quality control technique.

1. Introduction

Plasma spraying is a well established and versatile technique, and has been widely applied in modifying surface properties of metal components. Plasma spray coatings could have various functions such as improving wear resistance and thermal or chemical resistance. It may also improve special electrical, magnetic or decorative properties of the substrate. This type of coatings finds applications in many industries [1,2], e.g. thick coatings are applied in many industrial areas to restore or attain desired work piece dimensions and specifications.

Plasma spray coating characteristics are very dependent on spray parameters. According to some researchers [3] there are more than 50 macroscopic parameters that influence the quality of the coating. Depending on the application of plasma spray coating, different characteristics are important but there are some characteristics that are the same for all applications: thickness, porosity, microstructure, presence of unmelted particles, cracks and oxides, microhardness and bond strength. The poor bonding between splats and the imperfections in the form of pores or thermal cracks cause the mechanical property values of plasma spray coatings to be considerably lower than those of the corresponding monolithic materials [4]. Evidently the quality of a thermal spray coating is, to a large extent, determined by the quality of its adhesion between the coating and the underlying substrate as well as its cohesion among splats, i.e. adhesion/cohesion bond strength [1,5,6]. Adhesion bond strength primarily determines the quality of a coating while the cohesion bond strength indicates coating wear behavior.

There are a large range of available laboratory test methods for the evaluation of the thin or thick coatings adhesion/cohesion bond strength [1,5,7,8]. However none of them may be regarded as ideal, and all of them have certain advantages and disadvantages. Moreover, the results obtained are hard to be compared. Compared to other methods, the scratch test is fairly reliable, simple to use and no special specimen shape or preparation is required [9]. In addition, scratch testing is very useful for optimization of plasma spraying parameters [10]. The scratch test has been used for many years to provide a measure of coating/substrate adhesion [11], and determination of adhesive and other mechanical failure modes of thin coatings (up to 20 μm) by scratching the coatings surface has already been standardized [12].

Recently there have been attempts to determine the adhesion of thermal spray coatings by using scratch tests for thick coatings

☆ The paper was originally presented at the World Tribology Congress 2009 (WTC IV) Kyoto, Japan, 6th–11th September 2009.

* Corresponding author. Tel.: +381 11 33 02 291; fax: +381 11 33 70 364.
E-mail addresses: avencl@mas.bg.ac.rs (A. Vencl), saioa.arostegui@csm-instruments.com (S. Arostegui), gregory.favaro@csm-instruments.com (G. Favaro), zivic@kg.ac.rs (F. Zivic), miki@insimtel.com (M. Mrdak), boban@kg.ac.rs (S. Mitrović), vpopovic@mas.bg.ac.rs (V. Popovic).

0301-679X/$ - see front matter © 2011 Elsevier Ltd. All rights reserved.
doi:10.1016/j.triboint.2011.04.002

in the same manner as in the thin coatings, i.e. scratching on the top surface of the coating with constant or increasing load. However, due to a much higher thickness and surface roughness of thermal spray coatings the method has been found to be unsatisfactory [13]. In order to solve this problem a new method first introduced by Lopez et al. [14] that consists of running a constant load scratch test on a cross-section of the coating was proposed by ISO [15].

This paper analyzes the possibility of adhesion/cohesion bond strength evaluation of the thick plasma spray coatings by scratch testing on coatings cross-sections, according to the ISO working draft (ISO/WD 27307), and compares it to the most commonly applied standard tensile test method for adhesion or cohesion strength of thermal spray coatings (ASTM C 633). Both tests belong to the mechanical methods group [5] in which the adhesion is determined by the application of a force to the coating/substrate system. Materials used in the tests were four different plasma spray coatings whose bond strengths were measured by both test methods, compared and discussed.

2. Experimental details

2.1. Materials

Four spray powders were used in the experiment: two ferrous based powders (Sulzer Metco 4052 and Metco 92F), one molybdenum based powder (Metco 505) and one tungsten carbide–cobalt based powder (Metco 34F). The chemical compositions of the powders are shown in Table 1.

The Sulzer Metco 4052 powder is made of slightly alloyed steel, processed by gas atomization. It shows fine spherical morphology with particle granulation $-38/+15$ μm. Metco 92F is a fine grade of high carbon iron powder, processed by water atomization, which shows irregular morphology with particle granulation –53/+10 μm. The Metco 505 powder is a blend of molybdenum and nickel–chrome self-fluxing alloy. The share of the individual powder in the blend was 75 wt% of molybdenum and 25 wt% of nickel–chrome self-fluxing alloy. This spray powder blend shows spherical morphology with particle granulation –90/+15 μm. The Metco 34F powder is composed of a fine tungsten carbide–cobalt powder blended with a fine nickel–chrome self-fluxing alloy powder. It contains 50 wt% of tungsten carbide–cobalt and 50 wt% of nickel–chrome self-fluxing alloy. Particle granulation of this spray powder blend was $-53/+15$ μm.

The substrate material for the first two ferrous based coatings was a Al–Si alloy (EN AlSi10Mg), which was produced using sand casting followed by solution annealing at 540 °C with 35 °C/h, water quenching and artificial ageing at 160 ± 5 °C for 6 h. The substrate material for the other two coatings (molybdenum based and tungsten carbide–cobalt based) was a stainless steel (EN X15Cr13). This substrate material was used without any heat treatment. For the convenience, coatings attained using Sulzer Metco 4052, Metco 92F, Metco 505 and Metco 34F powders are hereafter referred to as 4052, 92F, 505 and 34F, respectively.

A deposition of all coatings was done by atmospheric plasma spraying (APS) process. Coatings 4052 and 92F were deposited with a Metco 7MB plasma spray gun, while coatings 505 and 34F were deposited with a Plasmadyne SG-100 plasma spray gun. In both cases specimen holder was rotated at constant speed of 500 mm/s while the traverse speed of a spraying gun was maintained constant at 4 mm/s. Before the spraying process, the surface of the substrate was activated and preheated. Activation (roughening) was done with an appropriate abrasive. The target coating thickness for all specimens was 350–400 μm. The selected spray parameters are given in Table 2.

2.2. Microstructure analysis and indentation tests

Metallographic samples were prepared in a standard way applying grinding and polishing with no etching, where the coatings were sectioned perpendicular to the coated surface. The microstructure of the coatings and presence of the cracks were analyzed with an optical microscope (OM) and a scanning electron microscope (SEM). Characterization was done according to the Pratt & Whitney standard [16].

Indentation tests of the obtained coatings included hardness, modulus of elasticity and plasticity measurements and measurements were made on the cross-sectional surface of the coatings (perpendicular to the coated surface). These tests were carried out using a CSM micro-indentation tester and applying the Instrumented indentation technique [17,18]. The Instrumented indentation technique is described in detail in the appropriate ISO 14577 standard.

The micro-indentation tester uses an already established method where an indenter tip with a known geometry is driven into the specific site of the material to be tested, by applying an increasing normal load. When reaching the pre-set maximum value, the normal load is reduced until partial or complete relaxation occurs. At each stage of the experiment the position of the indenter relative to the sample surface is precisely monitored with a differential capacitive sensor. With the constant multicycle mode, which is used in tests, indents are repeated in the same place several times (cycles) in order to provide information about the fatigue behavior of the coating. This procedure was performed in ambient air, at the temperature of 23 °C and

Table 2
Selected APS spray parameters values used for coatings deposition.

Spray parameter	Coating			
	4052	92F	505	34F
Primary plasma gas, Ar (l/min)	100	80	47	47
Secondary plasma gas, H_2 (l/min)	5	15	10	12
Electric current (A)	500	500	500	500
Powder carrier gas, Ar (l/min)	37	37	5	4
Powder feed rate (kg/h)	2	4.5	2.4	1.8
Spray distance (mm)	150	75	130	125

Table 1
Chemical composition of used powders in wt%.

Powder[a]	C	Mn	Mo	WC12Co	Ni	Cr	B	Si	Fe
Sulzer Metco 4052	1.2	1.5	–	–	0.3	1.3	–	–	Balance
Metco 92F	3.5	0.35	–	–	–	–	–	–	Balance
Metco 505	0.2	–	75	–	Balance	4.25	0.8	1.0	1.0
Metco 34F	0.5	–	–	50	33	9	2.0	2.0	3.5

[a] Commercial brand names of Sulzer Metco Inc. and Metco Inc.

humidity of 40%. The following indentation parameters were used to produce two multicycle indents on each sample: indenter Vickers; contact load 10 mN; constant loading rate 5 N/s; maximum load 15 N; reduced load (unload value) 5 N and number of cycles 100 cycles (see Fig. 5).

The indentation hardness, H_{IT}, is defined as the mean contact pressure and is given by

$$H_{IT} = \frac{F_{max}}{A_p} \text{ (MPa)},$$

where F_{max} is the maximum normal load (Fig. 1) and A_p is the projected contact area at that load. For better comparison of the results indentation hardness was converted to the Vickers hardness, *HV*. For a Vickers indenter the angle between the axis of diamond pyramid and its faces is $\alpha = 68^\circ$, so we have the following relation:

$$HV = 0.0945 H_{IT}.$$

The indentation modulus, E_{IT}, is calculated from the slope of the tangent of the unloading curve (Fig. 1)

$$E_{IT} = \frac{1-\nu_s^2}{(1/E_r)-(1-\nu_i^2/E_i)} \text{ (GPa)},$$

where E_i is the elastic modulus of the indenter (1141 GPa for diamond), ν_i is Poisson's ratio of the indenter (0.07 for diamond) and ν_s is Poisson's ratio of the tested sample. Determination of elasticity modulus was done under the assumption that all tested materials have Poisson's ratio of 0.3. The reduced modulus, E_r, which is calculated from the indentation data, is defined as

$$E_r = \sqrt{\frac{\pi S}{2\beta\sqrt{A_p}}} \text{ (GPa)},$$

where S is the contact stiffness ($S = dF/d\,Pd$, Fig. 1) and β is a geometric factor depending on the diamond shape, which in our case was square ($\beta = 1.012$). In order to compare the elastic properties of all samples, the parameter plasticity was defined and calculated from the following equation:

$$\text{plasticity} = \frac{Pd_{max} - Pd_1}{Pd_{max}}, \%,$$

where Pd_1 is penetration depth of first indent and Pd_{max} is maximal penetration depth (Fig. 1).

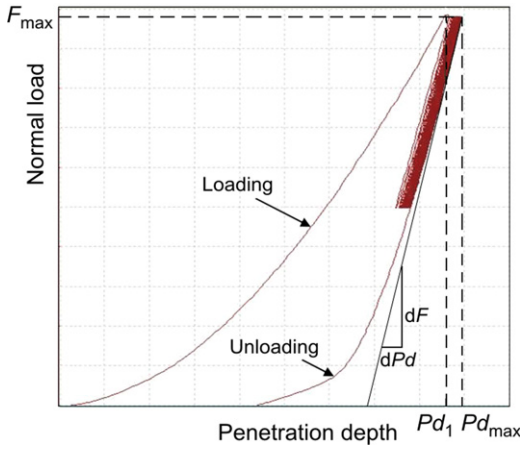

Fig. 1. Typical load vs. penetration depth curve for the Instrumented indentation technique constant multicycle mode.

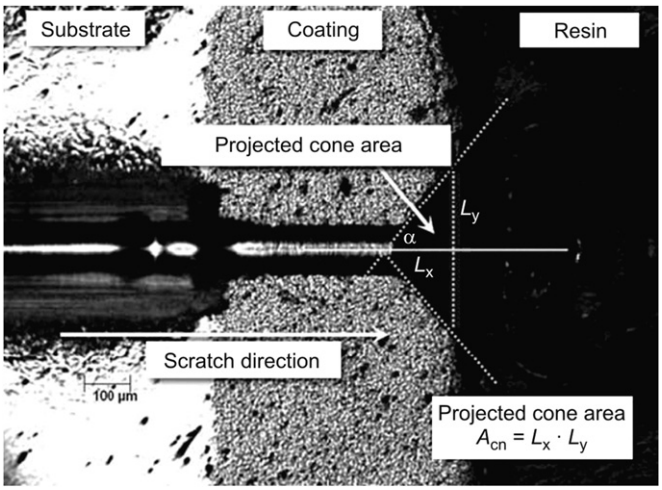

Fig. 2. OM images of the cone fracture area and nomenclature.

2.3. Adhesion/cohesion bond strength—tensile bond strength test (ASTM)

Tensile bond strength tests on the coatings were performed according to the ASTM C 633 standard. These tests were carried out using an Instron M 1185 hydraulic tensile test machine, applying cross-head velocities of 0.5 mm/min (coatings 4052 and 92F) and 1 mm/min (coatings 505 and 34F). The geometry of the specimens was cylindrical, Ø25 × 50 mm^2. Two specimens in pair were used, and the coating was deposited only on one of them. Specimens were bonded by glue and kept pressed against each other in a furnace. The bond strength was calculated by dividing the maximum (failure) load by the cross-sectional area of the specimen. The presented results of the coatings tensile bond strength tests represent an average value of a larger number of tests.

2.4. Adhesion/cohesion bond strength—scratch bond strength test (ISO)

Scratch bond strength tests on the coatings were performed according to the ISO/WD 27307 working draft. These tests were carried out using a CSM micro-scratch tester in ambient air, at the temperature of 23 °C and humidity of 40%. The following test parameters were used to produce three identical scratches on each specimen: indenter (stylus) type Rockwell diamond; stylus radius 50 µm; constant normal load 4 N; scratch length 0.7 mm and stylus velocity 1.4 mm/min. Specimens were embedded in resin and then polished in a standard way as metallographic samples. The scratch tests were carried out on cross-sections of the coatings and the stylus was slided from substrate towards the coatings.

During scratch bond strength tests, several data were measured and recorded such as normal, friction and critical force, coefficient of friction, and penetration and residual depth of the stylus. After the tests, the geometric values of the resulting cone-shaped fracture were also measured: cone length (L_x), width ($2 \ldots L_y$), and angle (α), and projected cone area ($A_{cn} = L_x L_y$; Fig. 2). Based on some other research [17] the projected cone area (A_{cn}) was chosen as the most characteristic factor for comparison, since it showed only a monotonic relationship to the scratching load.

3. Results

3.1. Microstructure and indentation tests results

The microstructures of the investigated coatings are shown in Figs. 3 and 4. The microstructures of all coatings were typical for

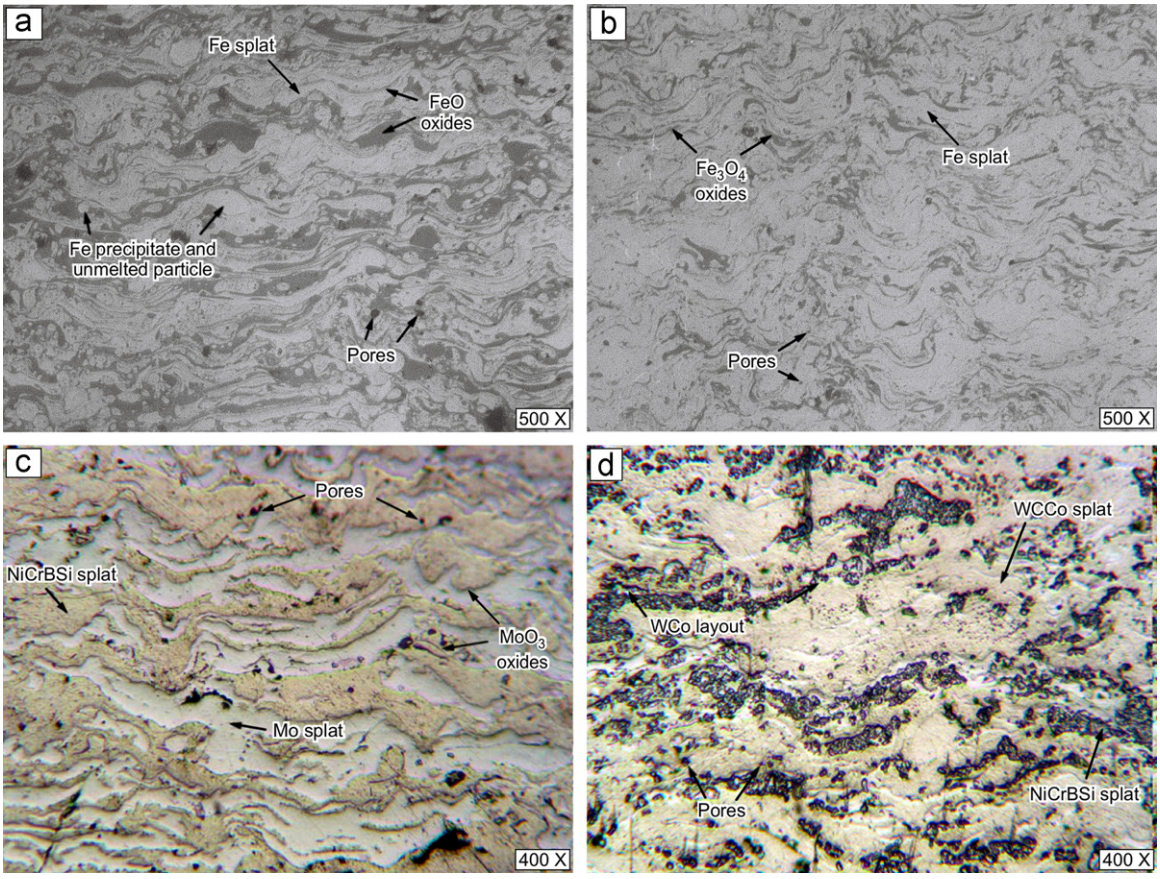

Fig. 3. Microstructures (OM) of the obtained coatings, no etching: (a) coating 4052, (b) coating 92F, (c) coating 505 and (d) coating 34F.

spray coatings and consisted of elongated splats of molten powder, which formed a curved lamellar structure, and oxide layers in between. No cracking was found in the coatings and no peeling was observed at the interface between the coating and the substrate. Also the distribution of coating thicknesses can be regarded as very stable.

The base of the coatings 4052 and 92F is formed by Fe layers. Oxide types between the Fe layers in these two coatings are revealed in some previous investigation [19] as FeO (coating 4052) and Fe_3O_4 (coating 92F). Based on the image analysis of OM micrographs, porosity of the coating 4052 was 5.8% with bigger pores of irregular shape (Fig. 3a) and porosity of the coating 92F was 2.3% (Fig. 3b). Presence of unmelted particles and Fe precipitates was detected only in coating 4052. In the coating 505 microstructure, two distinct layers could be clearly noticed (Fig. 3c). These are the Mo layers, which form a base of the coating, and the NiCrBSi layers, which are evenly distributed between the Mo layers. Inside the coating, there are fine and thin, dark colored MoO_3 oxide layers and micropores with the percent share of 3%. The presence of the unmelted particles in this coating was not noticed. Microstructure of the coating 34F was also lamellar and consists of WCCo and NiCrBSi layers. In the NiCrBSi layers, as a consequence of the mixing of WCCo and NiCrBSi powders, a light colored precipitates of WCo was noticed (Fig. 3c). Porosity of this coating was very low, and presence of the unmelted particles was not noticed.

On the SEM micrographs (Fig. 4) the structure of the obtained coatings is more obvious. For example these micrographs reveal that there was a porosity in the coating 34F, and that the porosity in the coating 4052 was much higher, approximately 30% (Fig. 4a). This porosity influenced the tensile test values and decreased the tensile bond strength.

The indentation test curves of the investigated coatings are shown in Fig. 5. In order to eliminate possible segregation effects and to get a representative values, two measurements were made for each sample. From Fig. 5 it can be seen that the results show good repeatability.

Indentation tests and measurements were made on the cross-sectional surface of the coatings (perpendicular to the coated surface; Fig. 6). These imprints and the applied load in the tests of 15 N indicate that the hardness is more in macro- than in micro-range. The summary of the obtained average values from the indentation tests is shown and discussed in a separate section (Table 5 in Section 4).

3.2. Adhesion/cohesion bond strength— tensile bond strength test (ASTM)

The values of tensile bond strength of the coatings obtained applying the ASTM C 633 standard are shown in Table 3. The value of the tensile bond strength for coating 4052 was lower than the expected value of 40–50 MPa, while the value for coating 92F was slightly higher than the prescribed value of 20.68 MPa. For the other two coatings (coatings 505 and 34F), the obtained values were in an acceptable range for this type of coatings.

Tensile bond strength depends on many parameters and some of the important ones are the amount of unmelted particles and pores in the coating and coating thickness. After a precise measurement of the coating thickness (six places on SEM micrographs), it was noticed that the thickness of the coatings 4052 and 92F was lower than the values prescribed by the standard of 0.38 mm. This influenced the tensile bond strength values of the coatings 4052 and 92F. The coating 4052 also showed high amount of pores (Fig. 4a). These facts also influenced the type of failure that occurred during the tensile tests (Table 3). According to the ASTM C 633 standard, there are three type

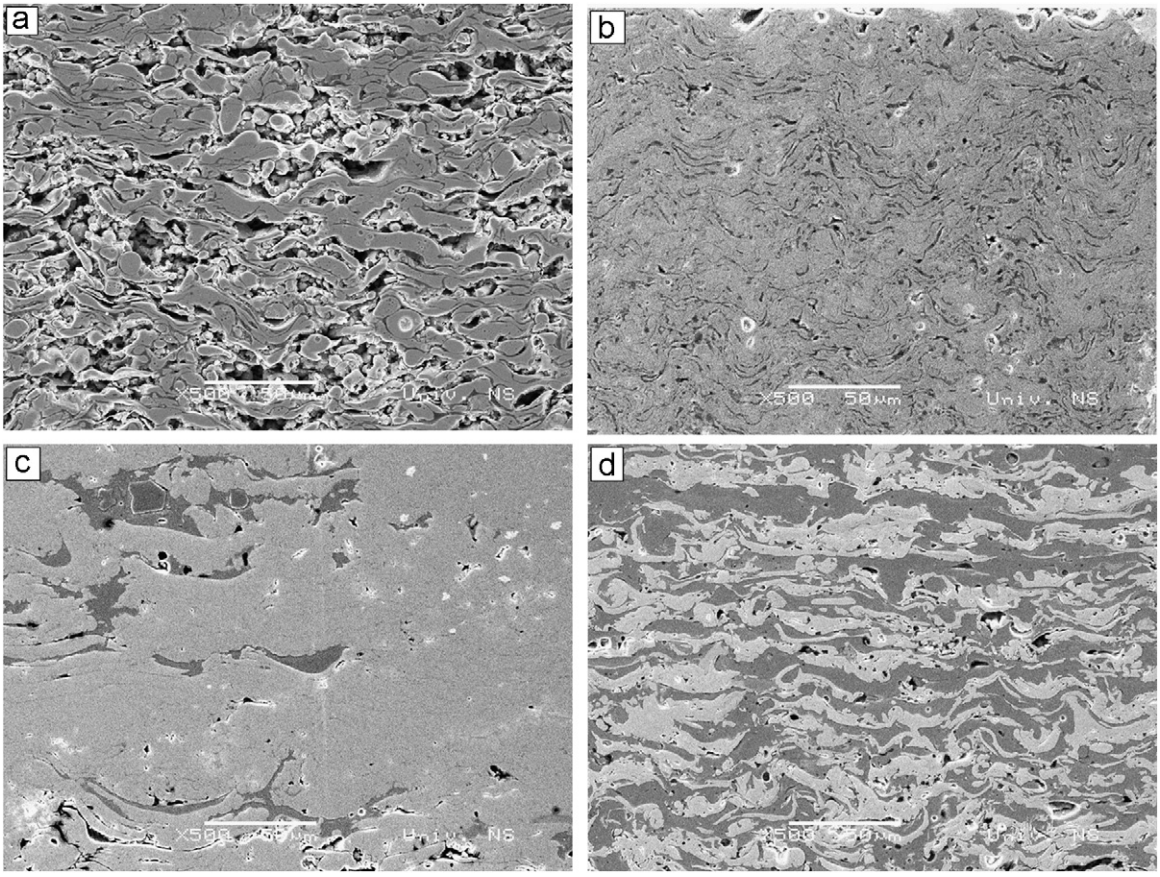

Fig. 4. Microstructures (SEM) of the obtained coatings, no etching: (a) coating 4052, (b) coating 92F, (c) coating 505 and (d) coating 34F.

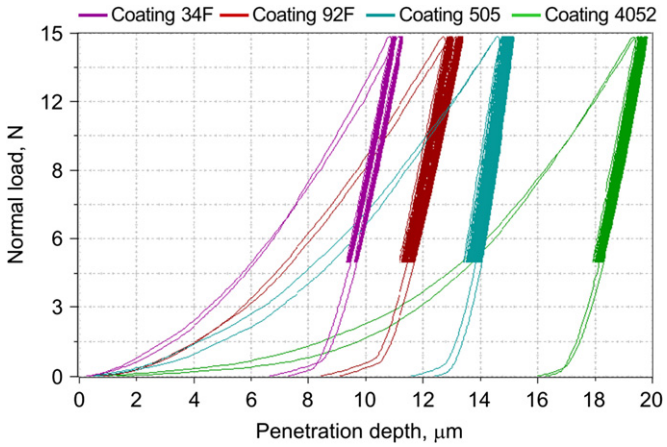

Fig. 5. Load vs. penetration depth curves of the investigated coatings.

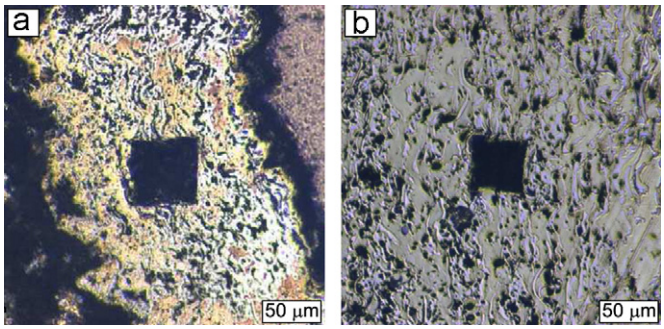

Fig. 6. Indentation test imprints: (a) coating 92F and (b) coating 34F.

Table 3
Averaged tensile bond strength test results of the investigated coatings.

Coating	Thickness (μm)	Tensile bond strength (MPa)	Type of failure
4052	270	26.61	Adhesive/cohesive
92F	230	31.08	Adhesive/cohesive
505	400	52	Adhesive
34F	360	59	Adhesive

of failures that can occur during the tensile test: adhesive, cohesive and a combination of these two (Fig. 7). For the coatings 4052 and 92F, during the tensile bond tests, the fracture occurred through the coating/substrate interface as well as through the coating layers (Fig. 8), which indicates weak cohesion strength between the layers. For the other two coatings (coatings 505 and 34F), the fracture, during the testing, occurred through the coating/substrate interface.

3.3. *Adhesion/cohesion bond strength— scratch bond strength test (ISO)*

The values of scratch bond strength of the coatings obtained applying the ISO/WD 27307 working draft are shown in Table 4. The coefficient of variation (V_r) of the projected cone area (A_{cn}) value was calculated as a standard deviation divided by the average value and multiplied by 100%. It is evident that the repeatability of the results of scratch bond strength test was average. The coating 4052 had the highest projected cone area value, which actually means the lowest scratch bond strength of this coating.

According to ISO/WD 27307 there are generally two types of failure that can occur during the test (Fig. 9): the cone-shaped

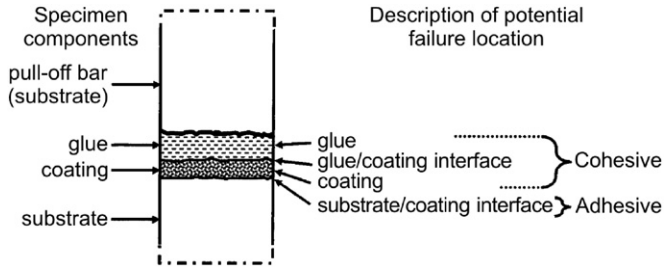

Fig. 7. Nomenclature of specimen components and classification of failure location for the tensile bond strength test.

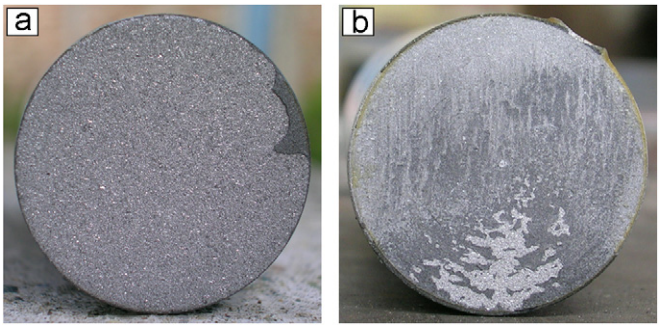

Fig. 8. Example of two types of failure for the tensile bond strength test (coating 4052): (a) adhesive and (b) cohesive.

Table 4
Averaged scratch bond strength test results of the investigated coatings.

Coating	Cone length L_x (μm)	Cone width $2L_y$ (μm)	Projected cone area $A_{cn} \times 10^{-3}$ (mm^2)	Coefficient of variation V_r (%)	Type of failure
4052	71.00	177.46	6.32	19.73	Cohesive
92F	51.03	117.48	3.00	16.63	Cohesive
505	30.45	89.83	1.37	18.27	Cohesive
34F	17.17	72.52	0.63	26.57	Cohesive

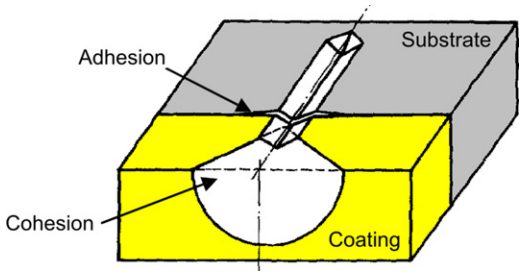

Fig. 9. Classification of the failure location for the scratch bond strength test.

fracture at the substrate/coating interface (indication of the coating adhesion) and the cone-shaped fracture in the coating (indication of the coating cohesion). As expected the cone-shaped fracture occurred on all the examined coatings (Fig. 10). Using the OM images after the scratch test it is very easy to indicate which type (adhesion/cohesion) of bond strength is critical for the observed coating. For all coatings the cone-shaped fracture occurs just inside the coatings, which reveals that the failure is due to a problem of cohesion within the coating itself (Table 4). Only on coating 505 small cracks were observed around the scratch, which decreased the values of the cohesive strength. These cracks are more obvious on the SEM image of the coating 505 scratch path (Fig. 11).

4. Correlation of the results and discussion

Four different thick plasma spray coatings were investigated in order to investigate the possibility of the adhesion/cohesion bond strength evaluation with scratch tester, by comparing it to the standard tensile test method. Since the higher projected cone area value actually means lower scratch bond strength of the coating, the parameter of inverted projected cone was used for the correlation of the two bond strength test results. The results of both tests, as well as the results of mechanical characteristics, are summarized in Table 5. For validation of the results, repeatability of the scratch bond strength test results must be considered since it was not the best one.

There have been some questions regarding the estimation of the brittle materials hardness using the Instrumented micro-indentation technique [20] but authors proved that if certain conditions (surface polishing, rigidity of samples and avoidance of cracks) are taken into consideration, it is possible to use this

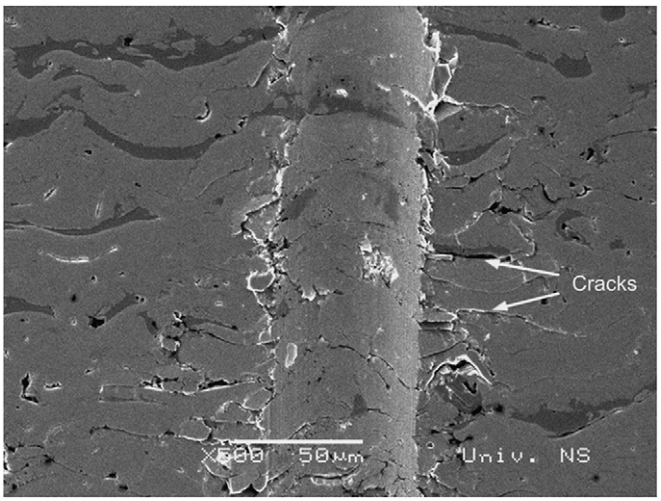

Fig. 11. Observed cracks around the scratch on the coating 505 (SEM).

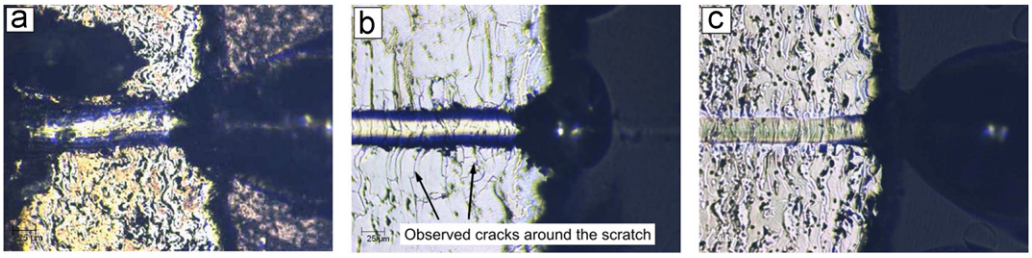

Fig. 10. Cone-shaped fracture occurring during the scratch bond strength test: (a) coating 92F, (b) coating 505 and (c) coating 34F.

Table 5
Mechanical characteristics and bond strength tests results of the investigated coatings.

Coating	Mechanical characteristics			Tensile test (ASTM)		Scratch test (ISO)	
	Hardness *HV* 1.5	Modulus of elasticity (GPa)	Plasticity (%)	Tensile bond strength (MPa)	Type of failure	Projected cone area invert value (mm^{-2})	Type of failure
4052	175	65.5	1.52	26.61	Adhesive/cohesive	158.19	Cohesive
92F	445	99	2.50	31.08	Adhesive/cohesive	333.61	Cohesive
505	299	118	3.31	52	Adhesive	730.65	Cohesive
34F	645	127	1.57	59	Adhesive	1592.90	Cohesive

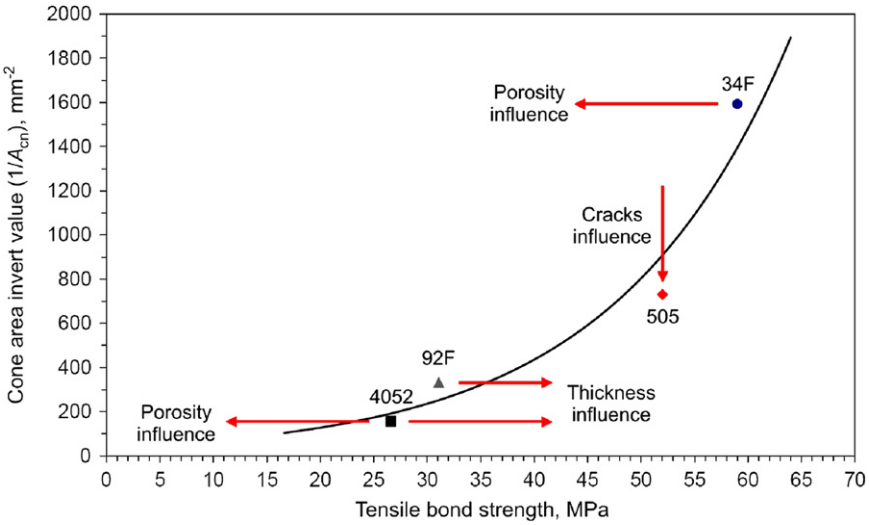

Fig. 12. Graphical correlation of the two bond strength tests and influencing parameters effects.

technique efficiently in characterization of brittle materials. One of the main requests imposed on the test is to apply indentation load lower than the value that produces cracks on imprints. Alcalá et al. [21] also emphasized that it is important to choose the indentation load in such a way as to avoid occurrence of microcracking at corners of the imprint. Since there were no cracks on the indentation test imprints (Fig. 6), it is obvious that the obtained values of hardness and elasticity modulus can be considered as appropriate for further analysis.

The first feature is that the hardness of the coating is not in correlation with either tensile or scratch bond strength values. This suggests that, for this type of materials, the Instrumented indentation hardness is not the best property for predicting the adhesion/cohesion bond strength. On the other hand, the modulus of elasticity was in correlation with the bond strength values of both test methods, i.e. higher modulus of elasticity implies higher tensile bond strength and higher scratch bond strength (Table 5). According to Hawthorne and Xie [22] the cohesive strength of plasma spray coatings includes many factors. Although some of these factors are difficult to measure individually, the cohesive strength of a material is closely linked to its resistance to contact deformation and its ability to deform without fracture [22]. This is in correlation with the obtained results since, for example, the coating 34F showed the highest values of elasticity modulus, i.e. resistance to contact deformation, and the highest values of the bond strength in both test methods as well. The plasticity for all coatings was very low, which is expected for brittle materials. There was a general trend between the tensile and scratch bond strength that coatings with higher tensile bond strength had higher scratch bond strength, but a direct comparison of the tensile and the scratch test results is questionable. A graphical interpretation of the relationship between two bond strength test results is shown in Fig. 12. It could be noticed that the relationship is more exponential than linear. There are small deviations of the measured values from the theoretical exponentional curve, first of all due to the coating deposition process parameters and secondly due to the observed failures during the tests.

Porosity generally decreases tensile test values since a pore of critical size can induce a macroscopic failure with tensile stress applied, while with compressive stress (scratch test) it is less influential. That is why the values of the cohesive tensile bond strength for coating 34F, and especially for coating 4052 (high porosity), are lower than expected (Fig. 12). Together with coating thickness smaller than the standard prescribed values, porosity could also increase the values of tensile bond strength since there is a possibility for glue to penetrate through the coating. Having this in mind and the fact that the thickness of coatings 4052 and 92F was smaller than it should be, it is possible that the tensile test values for these coatings are increased.

Microcracks, similar to the pores, can induce macroscopic failure when load of appropriate value is applied. Small cracks around the scratch path, observed after the test on the coating 505, decreased scratch test cohesive strength. For better correlation of the results more coatings should be tested while tribological tests (in dry and lubricated conditions) could also help in confirmation of the scratch test results (cohesion of the coatings).

5. Conclusions

After the characterization of the four different thick plasma spray coatings and examinations with scratch tester and with tensile test machine, some regularities could be established. First of all, it is confirmed that for this type of material, hardness is not the best property for predicting the adhesive/cohesive bond strength, which was expected.

A direct comparison of the tensile bond strength and the scratch test results is questionable although a general trend exists that a higher tensile implies a higher scratch bond strength. Moreover the type of failures for these two test methods was different for the same coating.

The scratch test is a relatively easy and quick test method and it could be easily used for indicating which type (adhesion/cohesion) of bond strength is critical for the observed coating. So far scratch test seems to be an efficient method for characterization of the thick coatings cohesion. For the practical application scratch test, being basically a comparison test, can be used as a supplement to some standard test method, and as a quality control technique.

Acknowledgements

This work has been performed within the Projects TR 35021 and TR 34028. These projects were supported by the Republic of Serbia, Ministry of Science and Technological Development, whose financial help is gratefully acknowledged.

References

[1] Heimann RB. Plasma-spray coating: principles and applications. Weinheim: VCH Verlagsgesellschaft mbH; 1996.
[2] Koutsomichalis A, Vaxevanidis N, Petropoulos G, Xatzaki E, Mourlas A, Antoniou S. Tribological coatings for aerospace applications and the case of WC–Co plasma spray coatings. Tribology in Industry 2009;31(1–2): 37–42.
[3] Lugscheider E, Barimani C, Eckert P, Eritt U. Modeling of the APS plasma spray process. Computational Materials Science 1996;7(1–2):109–14.
[4] Erickson LC, Westergård R, Wiklund U, Axén N, Hawthorne HM, Hogmark S. Cohesion in plasma-sprayed coatings—a comparison between evaluation methods. Wear 1998;214(1):30–7.
[5] Bull SJ, Rickerby DS. Characterization of hard coatings. In: Bunshah RF, editor. Handbook of hard coatings. Park Ridge: Noyes Publications; 2001. p. 181–228.
[6] Leigh SH, Berndt CC. A test for coating adhesion on flat substrates—a technical note. Journal of Thermal Spray Technology 1994;3(2):184–90.
[7] Lacombe R. Adhesion measurement methods: theory and practice. Boca Raton: CRC Press; 2006.
[8] Bouzakis K-D, Asimakopoulos A, Michailidis N, Pavlidou E, Erkens G. The inclined impact test, an efficient method to characterize coatings cohesion and adhesion properties. Tribology in Industry 2005;27(1–2):3–11.
[9] Vencl A, Rac A, Ivković B. Investigation of abrasive wear resistance of ferrous-based coatings with scratch tester. Tribology in Industry 2007;29(3–4): 13–6.
[10] Zhang J, Chen H, Lee SW, Ding CX. Evaluation of adhesion/cohesion of plasma sprayed ceramic coatings by scratch testing. In: Marple BR, Hyland MM, Lau Y-C, Li C-J, Lima RS, Montavon G, editors. Thermal spray 2007: global coating solutions. Materials Park,: ASM International; 2007. p. 472–7.
[11] Bull SJ, Berasetegui EG. An overview of the potential of quantitative coating adhesion measurement by scratch testing. Tribology International 2006;39(2):99–114.
[12] EN 1071-3:2002. Advanced technical ceramics— methods of test for ceramic coatings— part 3: determination of adhesive and other mechanical failure modes by a scratch test; 2002.
[13] Nohava J, editor. Characterization of thermal spray coatings by instrumented indentation and scratch testing: part I. In: Applications Bulletin, no. 28. Peseux: CSM Instruments; 2009. p. 1–4. 〈http://www.csm-instruments.com/en/Characterization-of-thermal-spray-coatings-by-instrumented-indentation-and-scratch- testing_Part_I〉.
[14] Lopez E, Beltzung F, Zambelli G. Measurement of cohesion and adhesion strengths in alumina coatings produced by plasma spraying. Journal of Materials Science Letters 1989;8(3):346–8.
[15] ISO/WD 27307. Evaluation of adhesion/cohesion of plasma sprayed ceramic coatings by scratch testing.
[16] Standard Practices Manual (PN 582005). East Hartford: Pratt & Whitney; 2002.
[17] Randall N, editor. Overview of mechanical testing standards. In: Applications Bulletin, no. 18. Peseux: CSM Instruments; 2002. p. 1–4. 〈http://www.csm-instruments.com/en/tests-Standards〉.
[18] Franco Jr. AR, Pintaúde G, Sinatora A, Pinedo CE, Tschiptschin AP. The use of a Vickers indenter in depth sensing indentation for measuring elastic modulus and Vickers hardness. Materials Research 2004;7(3):483–91.
[19] Vencl A, Mrdak M, Banjac M. Correlation of microstructures and tribological properties of ferrous coatings deposited by atmospheric plasma spraying on Al–Si cast alloy substrate. Metallurgical and Materials Transactions A 2009;40(2):398–405.
[20] Petit F, Vandeneede V, Cambier F. Relevance of instrumented micro-indentation for the assessment of hardness and Young's modulus of brittle materials. Materials Science and Engineering A 2007;456(1–2):252–60.
[21] Alcalá J, Gaudette F, Suresh S, Sampath S. Instrumented spherical micro-indentation of plasma-sprayed coatings. Materials Science and Engineering A 2001;316(1–2):1–10.
[22] Hawthorne HM, Xie Y. An attempt to evaluate cohesion in WC/Co/Cr coatings by controlled scratching. Meccanica 2001;36(6):675–82.